Journal of Applied Fluid Mechanics, Vol. 16, No. 5, pp. 1044-1056, 2023.
Available online at www.jafmonline.net, ISSN 1735-3572, EISSN 1735-3645.
https://doi.org/10.47176/jafm.16.05.1546

Numerical Simulation and Validation of Flow-Induced Vibration of the Specific Rod under Elastic Supports using One-Way Fluid-Solid Interaction

R. Amirian[1], G. R. Zarepoor[1] and M. Talebi[2†]

[1] *Faculty of Mechanical Engineering, University of Guilan, Rasht, 4163-5184, Iran*
[2] *Reactor and Nuclear Safety Research School, Nuclear Science and Technology Research Institute, Tehran, 8146-1957, Iran*

†*Corresponding Author Email: mstalebi@aeoi.org.ir*

(Received September 18, 2022; accepted January 19, 2023)

ABSTRACT

The vibration induced by the cooling fluid flow around the fuel rods in the fuel Assembly of nuclear reactors causes the rods to be destroyed and eventually leak due to the fretting wear in the place of contact with their supports for a long time. In this paper, the vibration caused by axial fluid flow around a specific fuel rod under elastic supports is numerically simulated. In this study, the fluid flow is modeled using the Large Eddy Simulation (LES) turbulence model in the FLUENT software. The fluid-structure interaction is also modeled using the ANSYS coupling system. To validate the implemented numerical model, the test results of the reported brass rod vibration similar to the studied problem in this research are used. Due to the long execution time of the two-way fluid-structure interaction simulations with a high grid number, the one-way fluid-structure interaction method is proposed. The results of simulations show that the one-way fluid-structure interaction method can be used in cases where the vibration amplitude of the structure is less than the height of the viscous sub-layer. Also, this method reduces the simulation time by 80%. Finally, the results of the flow-induced vibration simulation of the fuel rod show that the vibration range of the fuel rod will increase by 20 times if the contact of the elastic supports with the rod is lost, which will lead to the intensification of the wear caused by the rod oscillation. Also, the main natural frequency of the rod decreases when the rod loses contact with the supports and falls within the range of the reactor excitation frequency, i.e. 0 to 50 Hz, which should be avoided.

Keywords: Flow-induced vibration; One-way fluid-structure interaction; LES turbulence model; Fuel rod; Elastic supports.

NOMENCLATURE

c	damping	$\tilde{u}$	velocity field
D_h	hydraulic diameter	y^+	dimensionless wall distance
f	force	z	axial coordinate
h	height of the first boundary layer	δ	Dirac delta function
i, j	tensor indices	θ	peripheral coordinate
k	stiffness	μ_t	viscosity of the sub-grid scale disturbance
m	mass	υ	kinematic viscosity
p	pressure	ρ	density
R	displacement vector	τ	sub-grid scale stress
$\dot{R}$	velocity vector	φ	flow parameter
$\ddot{R}$	acceleration vector	$\bar{\varphi}$	average variable
Re_D	Reynolds number	$\tilde{\varphi}$	large-scale variable
r	radial coordinate	φ'	fluctuating variable
S	rate of the tension tensor	Δt	time step
t	time	Δx	average third root of the cell volume

1. INTRODUCTION

Flow-induced vibration deals with the response of flexible structures exposed to fluid flow. Specifically, this term describes the relationship between fluid dynamic forces and damping or elastic forces in structures. Flow-induced vibration has been experienced in many fields, including the aerospace industry, power generation and transmission (thermal power plants and nuclear reactors), and submarine technology. Flow-induced vibration includes diverse and complex phenomena. Subcritical vibrations of the nuclear fuel assembly, the vibration of pipes containing fluid, and the rotational movement of heat exchanger tubes are typical examples of this phenomenon.

An axial flow induces transverse vibrations with a smaller amplitude than transverse flow to the structures. This range is so small that it poses few problems in some cases. However, in some applications such as fuel rods in nuclear reactor fuel assemblies and tubes in heat exchangers where the flow is predominantly axial, it can be problematic. In this case, the problem arises due to the close space between the cylinders or the space between the cylinders and the supports. Therefore, even a low vibration amplitude can cause damage to cylindrical structures by causing (intensification) wear due to oscillation (Païdoussis 2004). Therefore, unlike transverse flow vibration problems, low-amplitude axial flow vibration problems usually become prominent after a long time and destruction due to alternating stresses. Another important reason for paying attention to the axial flow-induced vibration is that in some structures, due to the type of materials used, the structure of the supports or their dimension is flexible and prone to vibrations with a larger amplitude (Païdoussis 2004).

The most important parts of the fuel assembly are fuel rods and their spacer grids (Fig. 1). The rods are supported by the spacer grids at specific intervals. In pressurized water power plants, the heat produced by the rods is absorbed by pressurized water, called cooling, and transferred to the second cycle fluid in heat exchangers. In a nuclear power plant, the coolant must absorb as much heat as possible to achieve the highest possible output power. This feature is obtained by the high speed and turbulence of the cooling fluid flow. The vibration of the rods caused by the fluid flow and the wear phenomenon caused by the vibration appears as the most significant damage. Therefore, to increase the power of fuel assemblies, it is necessary to know the vibration behavior of the rod. During operation in the reactor, the contact force between the rod and the supports is reduced, and a gap may be created between them. This phenomenon, known as spacer relaxation, occurs due to the decrease in the spring rate of the spacers, the increase in the diameter of the spacer, and the decrease in the diameter of the rod (Kim 2010). As a fundamental principle in the design of components that are under dynamic load, the excitation frequency must be far enough away from the range of natural frequencies so that it does not suffer from an increase in the range of oscillation and

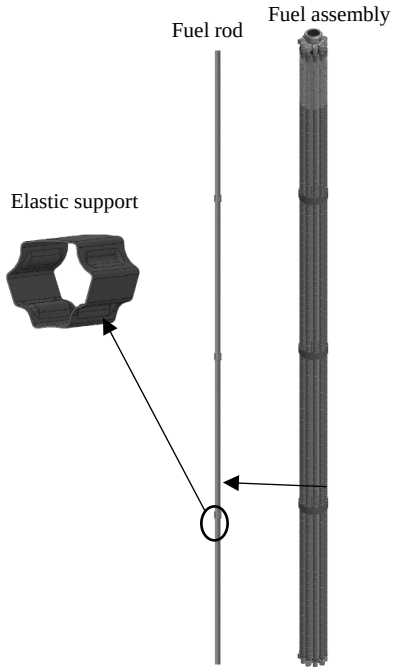

Fig. 1. Studied nuclear fuel assembly and its components.

finally does not get destroyed over time (Païdoussis 1983; Kim 2010). According to the report of the International Atomic Energy Agency, between 2006 and 2015, about 57% of the reported leaks in power reactors were due to the fretting wear between rods and spacers (IAEA Nuclear Energy Series No. NF-T 2019).

In international scientific centers, many studies have been carried out in the field of flow-induced vibration of cylindrical structures (Chen 1987; Païdoussis 1998, 2004). Much research studies have been done in the nuclear industry support centers on the axial flow-induced vibration of fuel rods. Initially, these investigations paid attention to extracting theoretical relationships, laboratory tests, and extracting experimental relationships. One of the earliest studies in this field was conducted by Païdoussis (1965). He modeled the fuel rod as an Euler-Bernoulli beam between two simple fixed supports. Then Kanazawa (1969) simplified the fuel rod motion equation. His two subsequent studies (Païdoussis 1974, 1969;) presented a semi-empirical relationship for estimating the vibration amplitude due to flow in such structures, which is still in use.

The phenomenon of flow-induced vibration in fuel rods has been studied in out-pile test equipment and numerically modeled since the early 90s. To model the vibration response of the fuel rod to the turbulent fluid flow, some computer codes have been developed and used to calculate the response of the fuel assembly with actual dimensions (IAEA-TECDOC-1454 2004).

Many studies have been done in numerical simulation of the flow-induced vibration of fuel rods using the structure-flow interaction model. In his research, Zhang (2011) investigated experimentally

and numerically the vibration of CANDU fuel assembly subjected to turbulent flow. The three-dimensional turbulent flow along the assembly was simulated using the LES model, and the results were validated with experimental data. In his PhD thesis, Liu (2012) carried out a numerical simulation of the fluid-structure interaction with the finite element method for a cylinder and a set of multiple flexible cylinders in a limited axial flow to estimate the vibration caused by the flow. Wu *et al.* (2014) experimentally investigated the vibration behavior of fuel rods caused by leakage flow. De Ridder *et al.* (2013) numerically modeled the vibration behavior of a flexible rod subjected to axial flow. They solved the averaged Navier-Stokes equations for incompressible fluid by finite volume method and using FLUENT software. Then De Ridder *et al.* (2016)

simulated the vibrations caused by the turbulence in the annular axial flow using the LES turbulence model. De Santis and Shams (2017) in their research have compared the numerical results of the flow-induced vibration in two different end conditions of the rod with the laboratory test results. Nazari *et al.* (2019) simulated the flow-induced vibration of a long cylindrical rod using the two-way structure-fluid interaction method and the LES model in FLUENT software. They investigated grid independence study only in radial direction and the simulation is significantly different from the benchmark results. This problem has been solved in the current research by implementing a grid independence study in all directions.

A Survey in the literature review shows that the flow-induced vibration simulation of the fuel rod without considering the effect of the rod supports and using the two-way fluid-structure interaction method has a high computational cost. The previous research of the authors of this article showed that these elastic supports have a significant effect on the vibration behavior of the rod (Amirian *et al.* 2022). Therefore, in this research, the vibrations caused by the axial flow of a particular fuel rod have been studied to investigate the effect of these supports on the vibration of the rod. For this purpose, firstly, the method of modeling the structure-fluid interaction is described, and then validated using the brass rod test results reported in reference Chen and Wambsganss (1972). Also, in this research, considering the hardware limitations and long simulation time using the two-way fluid-structure interaction method, the possibility of using the one-way interaction method has been investigated. Finally, the amplitude and frequency of the flow-induced vibration of the studied fuel rod are simulated and analyzed in two cases, with and without the supports.

2. GOVERNING EQUATIONS AND SOLUTION METHOD

2.1 Governing Equations

When the Reynolds number exceeds a specific limit, the flow will become turbulent. Turbulent flow is characterized by oscillation and disturbance. Although the Navier-Stokes equations governing fluid motion can estimate flow behavior by considering disturbance, it takes too much computational cost to simulate and solve such fluctuations. Such an approach is called direct numerical simulation. An alternative method is to add the disturbance effect with the help of disturbance models. In this approach, the variables in the Navier-Stokes equation are divided into average ($\bar{\varphi}$) and fluctuating ($\acute{\varphi}$) values. This operation is called Reynolds decomposition (Wilcox 1998). By placing the flow variables as $\varphi = \bar{\varphi} + \varphi'$ in the Navier-Stokes equations, the averaged Reynolds equations are obtained. These equations for incompressible fluid are obtained as follows:

$$\frac{\partial \bar{u}_i}{\partial x_j} = 0 \tag{1}$$

$$\rho\left(\frac{\partial \bar{u}_i}{\partial t} + \frac{\partial}{\partial x_j}\left(\bar{u}_i \bar{u}_j\right)\right) = -\frac{\partial \bar{p}}{\partial x_i} + \mu \frac{\partial}{\partial x_j}\left[\left(\frac{\partial \bar{u}_i}{\partial x_j} + \frac{\partial \bar{u}_j}{\partial x_i}\right) - \frac{2}{3}\delta_{ij}\frac{\partial \bar{u}_i}{\partial x_i}\right] - \rho \frac{\partial}{\partial x_j}(\overline{\acute{u}_i} \tag{2}$$

Where i and j are tensor indices and δ_{ij} is the Dirac delta function. The expression $\rho \frac{\partial}{\partial x_j}(\overline{\acute{u}_i \acute{u}_j})$ is called the Reynolds stress, and due to its unknown nature, the above equations cannot be solved directly for turbulent flows. Methods have been developed to solve Reynolds stresses, the most famous of which are K-ε or K-w.

If these models are used, the obtained vibrations will be damped and only parameters such as the oscillation frequency, and the damping coefficient of the structure can be obtained (Ter Hofstede *et al.* 2017; Nazari *et al.* 2019). This result is predictable, considering that the mentioned models solve the Reynolds averaging equations and do not model the fluctuations of variables such as pressure and velocity. In this case, the pressure function that is applied the structure (just like an initial excitation) is symmetric. After over time, it is damped due to the absence of fluctuations caused by disturbances. However, if the purpose of vibration simulation is to obtain the parameters such as the amplitude of the oscillations or the pressure distribution function on the structure, it is necessary to use models that can solve the very small disturbances caused by the viscosity near the wall. One of these models is the LES turbulence model, which has a higher computational cost, but it is less than the computational cost of the direct method.

The governing equations in the LES method are the averaged Navier-Stokes equations in three-dimensional space relative to the grid size (Wilcox 1998). The conversion process effectively recovers eddies whose sizes are smaller than the scale width or cell space. The resulting equations also control the dynamics of large eddies. Each variable in the flow

is broken into two large-scale and sub-grid scale: $\varphi = \tilde{\varphi} + \varphi'$. The transformed Navier-Stokes equations for incompressible flow are obtained as follows:

$$\frac{\partial \tilde{u}_j}{\partial x_j} = 0 \tag{3}$$

$$\frac{\partial \tilde{u}_i}{\partial t} + \frac{\partial}{\partial x_j}\left(\tilde{u}_i \tilde{u}_j\right) = \nu\left(\frac{\partial^2 \tilde{u}_i}{\partial {x_j}^2}\right) - \frac{1}{\rho}\frac{\partial \tilde{p}}{\partial x_i} + \frac{\partial \tau_{ij}}{\partial x_j} \tag{4}$$

Where $\tilde{u}_i$ is the velocity field, and τ_{ij} is the subgrid-scale stress. Many of the subgrid-scale models use eddy viscosity models as follows:

$$\tau_{ij} - \frac{1}{3}\delta_{ij}\tau_{kk} = -2\mu_t S_{ij} \tag{5}$$

Where μ_t is the viscosity of the sub-grid scale disturbance, and S_{ij} is the rate of the tension tensor for the solvable scale.

The equation governing the motion of a multi-degree-of-freedom system is given below:

$$m\ddot{R} + c\dot{R} + kR = F(t) \tag{6}$$

In this relation, m is the mass matrix of the structure, $\ddot{R}$ is the acceleration vector, c is the damping matrix of the structure, $\dot{R}$ is the velocity vector, k is the stiffness matrix of the structure, R is the displacement vector, F is the force vector which is a function of time. It should be noted that the above equation can be achieved by applying Navier's equation to the elements of the structure and aggregating them.

2.2 Fluid-Structure Interaction

It is usually complicated to solve theoretical problems involving several environments (multiphysics). Therefore, they should be solved either numerically or experimentally. Today, several commercial software makes the numerical solutions to these problems possible. There are two different approaches to solving fluid-structure interaction problems numerically. If the deformation of the structure has a negligible effect on the fluid flow, only the effect of the fluid on the structure can be solved, called one-way interaction. If the deformation of the structure affects on the fluid flow, the effect of the structure on the fluid should also be considered, which is called two-way interaction.

According to the authors' experience and the results of existing researches, it is too clear that the disturbance of the flow is the cause of vibration in the rod. Also, the review of the research background shows that the FUENT software, as one of the ANSYS software modules, is capable of modeling flows with permanent disturbances in the fluid flow field with the help of the LES turbulence model. Therefore, in this research, the software available in ANSYS was used.

Table 1 Dimensions and physical properties of the fuel rod.

property	value	Dimension (mm)	value
Young modulus (GPa)	95	Rod length	1200
Density (kg/m^3)	6550	Rod diameter	9.1
Poison ration	0.4	Spacer intervals	300

Table 2 Characteristics of fluid flow.

Property	value
Fluid	Light water
Average inlet velocity (m/sec)	4.5
Temperature (°C)	50
Outlet pressure (bar)	4

3. PROBLEM DEFINITION

3.1 Geometry of Studied Rod

To equalize the flow conditions (same Reynolds) for a rod in the fuel assembly, a channel with an equivalent hydraulic diameter has been used. The diameter of the channel is calculated to be 16 mm. The dimensions and physical characteristics of the fuel rod and the flow characteristics are given in Tables 1 and 2.

To complete the modeling of the rod, the modulus of rigidity and density must be determined. To consider the effect of pellets on the vibration behavior of the rod, the concept of equivalent density has been used, which is 22300 kg/m^3, according to the authors' previous research (Amirian *et al.* 2022). In addition, according to the research of Zargar *et al.* (2017), the modulus of rigidity or bending stiffness for the rod is almost the same in two conditions without and with pellets. That is, the pellets do not play any significant role in the bending of the rod within the vibration range of the rod (less than 50 microns) so its effect can be ignored.

According to the research of Nazari *et al.* (2020), the fuel rod is considered a thin-walled structure (with a thickness of approximately 0.7 mm), and due to the problems caused by the static deformation, which is the order of the vibration amplitude of the rod, the bar is used instead of the pipe. To equate the vibration behavior of an empty rod with a full rod, the characteristics affecting the structure's vibration, i.e., mass and modulus of rigidity, must be the same, and their outer diameter must be the same for the geometry exposed to the fluid. The density of the bar and Young's modulus are calculated at 6200 kg/m^3 and 45.5 GPa, respectively. The three-dimensional model of the fuel rod and the channel is given in Fig. 2.

To simplify the modeling of the supports, since the thickness of the support in the direction of the flow (about 0.25 mm) is small, it will not have a noticeable effect on the turbulence of the flow. Therefore, the support is modeled as virtual linear and bending elastic springs (Fig. 3). Stiffness coefficients of these

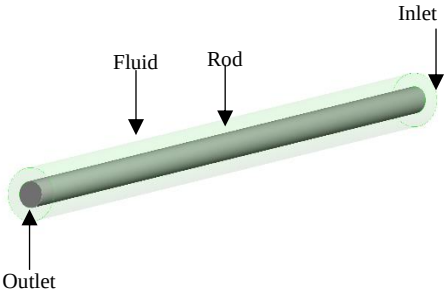

Fig. 2. Numerical model of the rod and the channel.

$$\begin{cases} r: \begin{cases} first\ layer: r^+ \sim 1 \\ viscous\ sublayer: r^+ < 5 \\ buffer\ layer: 5 < r^+ < 30 \\ Log - Law\ region: 30 < r^+ < 60 \end{cases} \\ \theta: \quad 15 \le (r\Delta\theta)^+ \le 50 \\ z: \quad 50 \le \Delta z^+ \le 150 \end{cases} \tag{7}$$

supports have also been obtained in the authors' previous research (Amirian *et al.* 2022).

3.1 Geometry of the Benchmark Problem

To validate the numerical model implemented to simulate fuel rod vibrations, a benchmark model of laboratory test results is available in Chen and Wambsganss (1972) research has been used. In terms of geometry and fluid conditions, this model is similar to the vibration model of this research, and only the material of the rod, and its fluid speed are different (Fig. 4). Geometric dimensions, physical properties of the rod and fluid conditions are given in Tables 3 and 4.

4. NUMERICAL SIMULATION OF FLOW-INDUCED VIBRATION

As mentioned, ANSYS software was used to solve the flow-induced vibration numerically. This software uses the coupling system module to solve the fluid-structure interaction problem. Different steps of simulation and solution methods are explained below.

4.1 Meshing

In general, one of the requirements of the LES method is that the meshing of the fluid medium in the entire computational domain is as close as possible to y^+ to reach more accurate solutions (Eggels 1995), in which case the number of meshes will be increased. Therefore, according to the hardware limitations, and time-consuming calculations, in order to achieve an accurate simulation and reduce the calculation time, the permissible range of grids has been proposed as follows (Piomelli and Chasnov 1996; Wilcox 2006; Georgiadis *et al.* 2010):

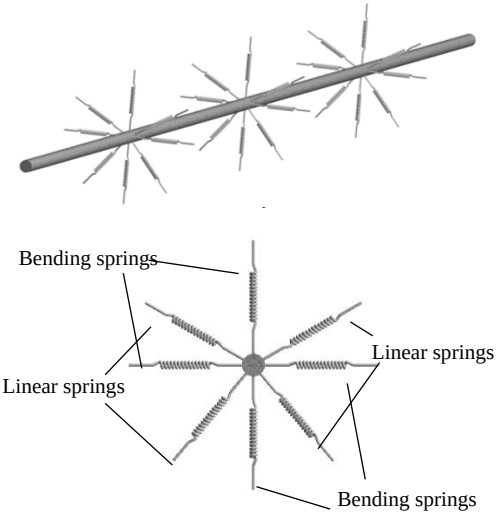

Fig. 3. 3D model of the fuel rod with spring supports.

Table 3 Dimensions and physical properties of the benchmark problem.

property	value	Dimension (mm)	value
Young modulus (GPa)	107	Rod length	1190
Density (kg/m^3)	8400	Rod diameter	12.7
Poison ration	0.33	Channel diameter	25.4

Table 4 Characteristics of fluid flow.

Property	value
Fluid	water
Average inlet velocity (m/sec)	10
Temperature (°C)	20

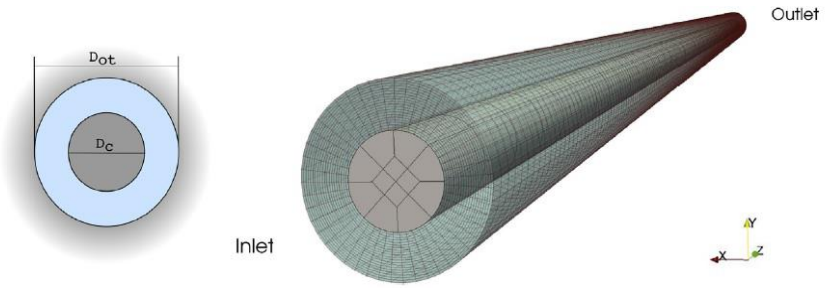

Fig. 4. Geometry of the Chen-Wambsganss model.

To estimate the thickness of the first boundary layer, the Blasius friction law is used for the flow inside the pipe (Lesieur 1997):

$$u_\tau = 0.164\ {}^{\upsilon}/_{D_h}\ {Re_D}^{7/8}$$
$$\Delta x = \frac{h}{2} = {}^{\upsilon}/_{u_\tau}\ y^+ \tag{8}$$

Where u_τ is the frictional velocity, D_h is the hydraulic diameter, υ is the kinematic viscosity, Re_D is the Reynolds number, and h is the thickness of the first boundary layer.

First, once the problem is solved with RANS models, and then by calculating of y^+, the number of grids in all three coordinates (radial, peripheral, and axial) can be determined to meet the permissible limits stated in Eq. (7). Also, using the meshing tools available in the software, meshing has been created according to the finite element method related to structural analysis. There is no need for the grid to be the same at the common boundary between the fluid environment and the structure. However, the point that has been gained from experience in this research and has not been mentioned in any other available research is that the width of the elements along the peripheral direction in both the fluid and the structure should be the same, distinctly. If the width of the elements is not the same in the peripheral direction, because the average force is applied in each element at its center, the angle of the resulting vector of the forces changes. Figure 5 shows a view of the meshing of the fluid and the structure.

4.2 Boundary Conditions

The end points of the rod are considered fixed in the inlet and outlet sections. The outer wall of the rod, which is exposed to the fluid, is considered the common boundary with the fluid. The boundary of the inner wall of the fluid changes due to the deformation of the structure. Therefore, this boundary is considered a dynamic boundary in the simulation of the interaction between the structure and the fluid. Other fluid boundaries are assumed to be fixed. The fluid inlet boundary is considered the velocity profile obtained from the RANS simulation, and the fluid outlet boundary is considered as constant pressure (zero gauge pressure).

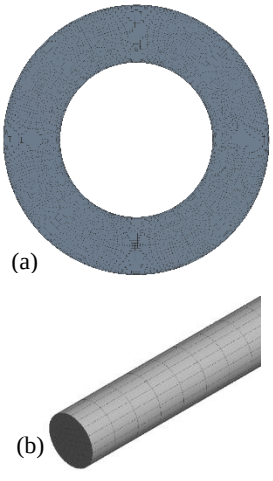

Fig. 5. Meshing of (a) fluid and (b) rod.

Considering that the LES model is a transient phenomenon, to reach a reliable solution, it is necessary to solve the fluid environment for a suitable time (usually 5 to 10 times the time that the fluid travels the length of the channel) so that the fluid parameters reach their stable values in the transient state. Then this solution is considered as the initial condition of the fluid.

4.3 Coupling Between Fluid Flow and Structure

As mentioned, in this research, due to the hardware limitations and long simulation time, using the two-way fluid-structure interaction method, the possibility of using the one-way interaction method has also been investigated. Determining the method of interaction between the structure and the fluid is based on the amplitude of the vibrations and the thickness of the viscous sub-layer. If the deformation of the structure is less than the height of the viscous sub-layer ($y^+ < 5$), the one-way method can be used, and if the deformation of the structure is greater than the height of the viscous sub-layer ($y^+ > 5$), the two-way method should be used. Finally, the time step is also calculated according to the fluid parameters and the definition of the Courant number (Sagaut 2001):

$$\Delta t = CFL * \Delta x/u \tag{9}$$

Where Δx is the average third root of the cell volume and u is the fluid velocity in that cell, and the Courant parameter (CFL) is less than unity (preferably 0.5). The time step of the problem can be obtained by solving the problem once and calculating the above formula in the entire domain. Table 5 shows the solution method used in these simulations.

5. FLUID FLOW SIMULATION USING LES MODEL

In this section, for the studied problem (with a shortened length of 1/4 of the original length of the channel), the fluid flow has been solved using the LES model. First, the problem is solved with the k-ε model, and then by calculating y^+, the number of grids in all three dimensions (radial, peripheral and axial) is determined to meet the permissible limits

Table 5 Solution method used in simulations.

Fluid solution method	PISO
Transient solution method	Second Order
Dynamic grid solution method	Smoothing, Diffusion
Sub-grid scale model	WALE
Inlet disturbance method	Vortex Method

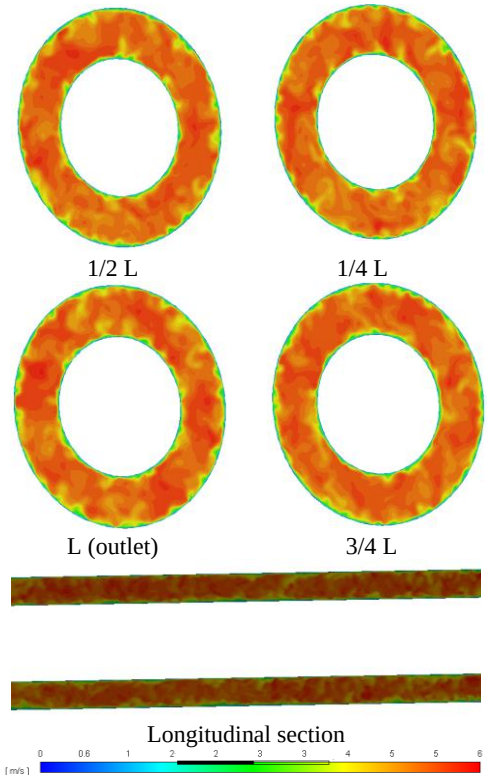

Fig. 6. Instantaneous fluid velocity contours.

stated in Eqs. (7). As explained in the previous section, to achieve a stable solution for the fluid flow, it is necessary to solve the fluid field for an enough time so that the fluid parameters reach their stable values in the transient state. The results of simulation of fluid flow after reach to stationary state are given below.

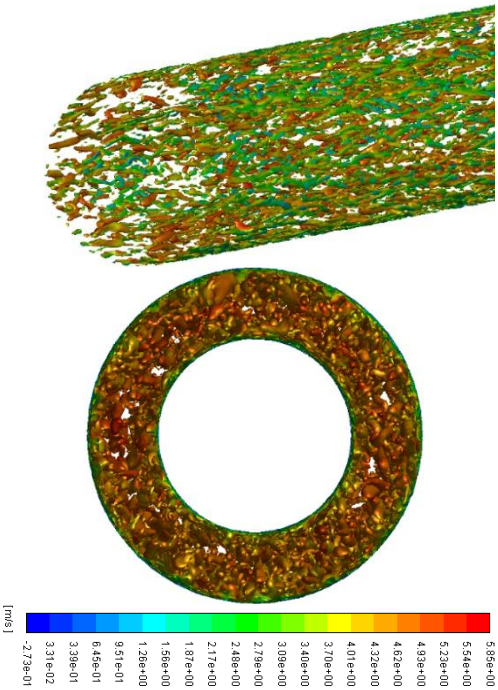

Fig. 7. 3d contours of eddies based on Q criterion colored by axial velocity.

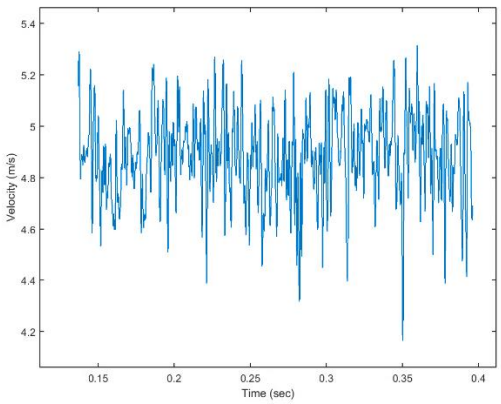

Fig. 8. Instantaneous velocity fluctuations at the midpoint of the fluid vs. time.

Figure 6 shows the velocity contour at different sections of the fluid channel. As expected, the value of the fluid velocity in the circumferential direction is completely asymmetric due to the flow fluctuations. One of the best parameter to show the turbulent vortical structures is the Q-criterion. Figure 7 shows eddies based on the Q-criterion. As can be seen, this simulation has been able to simulate the three-dimensional structure of the flow.

Figure 8 shows the instantaneous fluctuations of the velocity vs. time at the middle point of the channel. The amount of speed changes at this point is obtained in the range of 1 m/s.

5.1 LES Verification

To verify the fluid flow simulation using the LES model, two methods, the Kolmogorov theory and the LES quality index, have been used.

To ensure the adequacy of the grid filter, it is necessary according to the Kolmogorov theory, the slope of the intensity of the resolved turbulence kinetic energy in the inertial subrange is -5/3. Figure 9 shows the power spectral density diagram of turbulence kinetic energy in terms of the frequency at the middle point of the channel. The results show that based on the grid size up to a frequency of 2 kHz, the turbulence kinetic energy is well resolved.

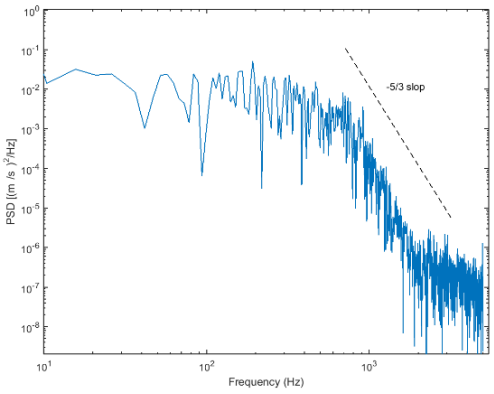

Fig. 9. Turbulence kinetic energy power spectral density diagram vs. frequency at the middle point of the channel.

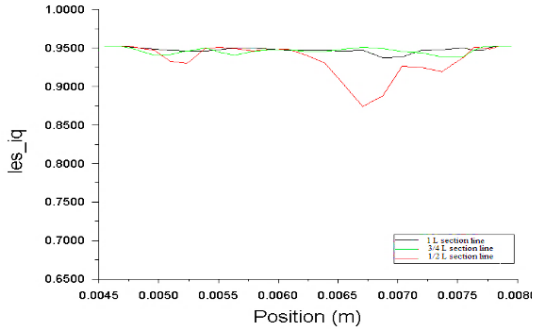

Fig. 10. LES quality index in the radial direction.

To verify the simulation, the LES quality index proposed by Celik *et al.* (2005) has been used. This index is the ratio of the resolved turbulence kinetic energy to the total turbulence kinetic energy. For most engineering applications, this index should be greater than 0.8. Figure 10 shows that the LES quality index for the simulated flow is about 0.95 in three different sections of the channel.

5.2 LES Validation

As mentioned, the main factor causing oscillation in the rod is the asymmetric pressure profile on the rod. The viscous forces normal to the cylinder are small and are thus neglected. Figure 11 shows the pressure contour in the middle section of the channel and on the middle outer surface of the rod. As seen, the amount of applied normal pressure is different along the circumference, and this issue causes oscillation in the rod. Figure 12 shows the pressure fluctuations vs. time at the middle point of the rod.

To validate the FIV simulation, the dimensionless wall pressure power spectrum density has been compared with the empirical models reported for annular flow geometry by Chen and Wambsganss (1972) and Wilson and Jones (1983). As seen in Fig. 13 at low frequencies, the constant pressure power density is consistent with the Wilson model, and for high frequencies, it is in good agreement with both models. Of course, the models mentioned in the range of low frequencies do not have valid experimental data and compared to the experimental data reported by Chen and Wambsganss (1972), the measured rms-displacement predicts more values. This can be attributed to the fact that turbulent boundary layer pressure variation is an important contributor to the measured vibration, but some far-field sound-induced vibration may also be present.

Therefore, according to the compatibility of the simulated wall pressure power spectrum density with the experimental results, the resulting displacement value will be at least of the order of the real displacement.

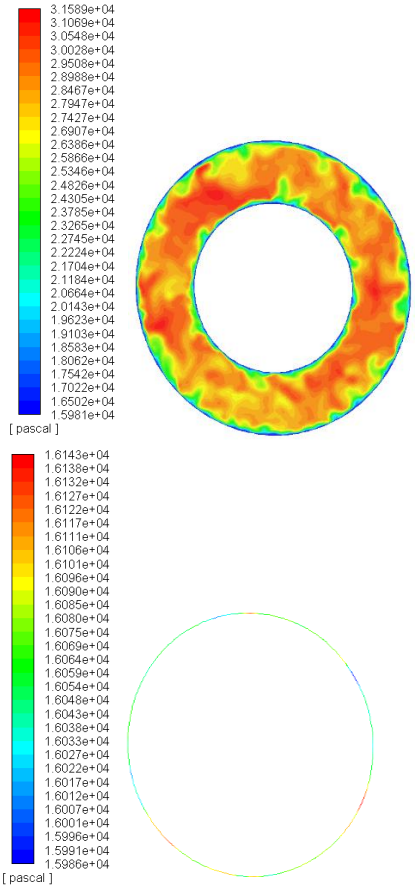

Fig. 11. Pressure contour in the middle section of the channel and on the middle outer surface of the rod.

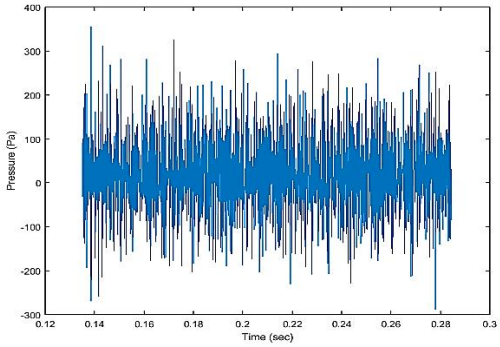

Fig. 12. Pressure fluctuations vs. time at the midpoint of the rod surface.

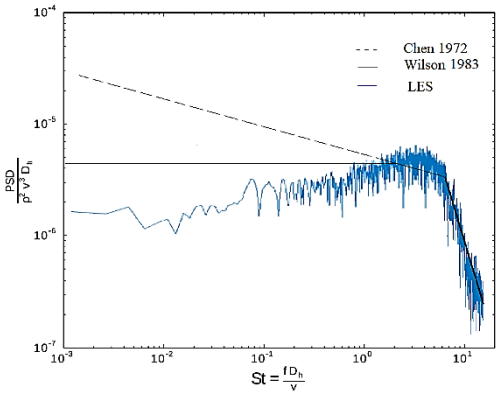

Fig. 13. Reduced Power spectrum density of the pressure vs. Strouhal number on the surface of the rod.

Table 6 Different types of meshing of brass rod fluid volume.

Mesh type	Number of divisions in (r, θ, z)	Number of meshes	Time step (msec)
coarse	(23,54,1600)	1987200	0.26
medium	(32,72,2000)	4608000	0.20
fine	(45,110,2000)	9900000	0.15
Extra fine	(40,150,2500)	17635000	0.13

6. SIMULATION RESULTS OF FLOW-INDUCED VIBRATION

Because the number of constituent elements in the LES model is significantly increased compared to the RANS models, a computer with high memory and processing speed is needed to perform the simulations. For this purpose, a computer with 28 cores and 128 GB of memory was used. To use all the cores simultaneously and increase the speed of simulations, parallel simulation was used.

6.1 Brass Rod Simulation Results

Based on Eqs. (8), the thickness of the first boundary layer to reach $y^+ \sim 1$ is 5 microns, and the time step is calculated based on Eqs. (9) for each mesh size. In order to achieve grid independence, the different types considered for meshing the fluid volume are given in Table 6.

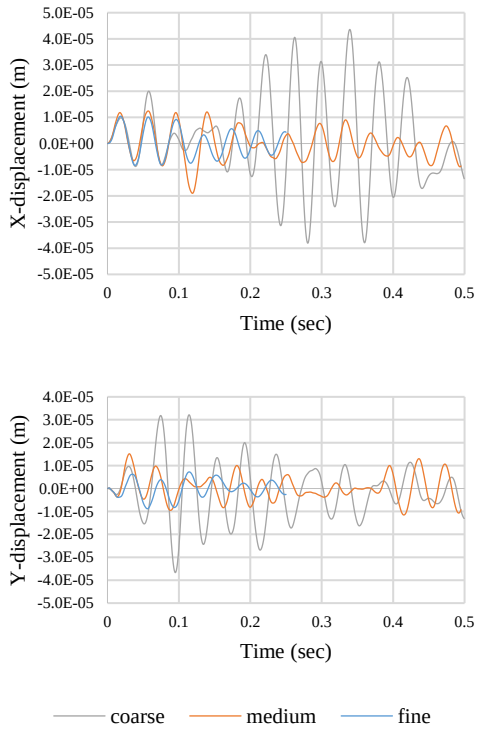

Fig. 14. Displacement vs. time of the middle point of the brass rod using two-way method.

6.1.1 Two-Way Fluid-Solid Interaction

It should be noted that because the vibration range of the rod is not initially known correctly, the two-way interaction method was used to ensure. The result of the two-way simulation shows that the range of the oscillation range is close to the thickness of the viscous sub-layer ($y^+ \cong 5$: about 30 microns). Figure 14 shows two-way simulations in several types of fluid volume meshing.

In Table 7, the frequency and rms-displacement of the brass rod are compared with the simulation results of Nazari *et al.* (2019) and reference experimental data and empirical model of Chen and Wambsganss (1972). As can be seen, with the increase in the number of grids, the average displacement of the rod is closer to the result of Chen and Wambsganss (1972), while the results of Nazari *et al.* (2019) have a significant difference from the benchmark results. In the present research, this problem has been solved by conducting a grid independence study, so that this difference has reached from 9 microns to less than 2 microns.

Table 7 Result of simulated and tested flow-induced vibration of the brass rod using two-way method.

Mesh type	Frequency (Hz)	RMS (μm)	Simulation time (days)
Coarse	24.5	21	5
Medium	26.5	11.5	10
Fine	25.8	6.5	25
Ref.			
Experiment (Chen and Wambsganss1972)	27.9	~5	-
Empirical model (Chen and Wambsganss1972)	30	~10	-
Simulation (Nazari *et al.* 2019)	26.9	13.7	-

6.1.2 One-Way Fluid-Solid Interaction

Considering the hardware limitations and long simulation time using the two-way fluid-structure interaction method (for example it takes about 45 days to simulate the extra fine mesh type, which is a lot of time), the possibility of using the one-way interaction method is investigated.

Figure 15 compares the one-way and two-way interaction methods for the coarse mesh type. The average displacement of the coarse mesh is 21.1 microns for the two-way mode and 24.5 microns for the one-way mode. Therefore, the one-way interaction method can be used with an acceptable

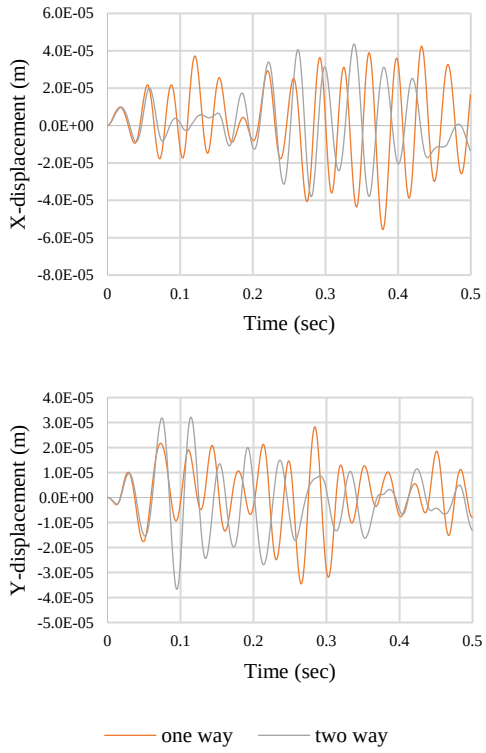

Fig. 15. Displacement vs. time of the middle point of the brass rod using two-way and one-way fluid-structure interaction for the coarse mesh.

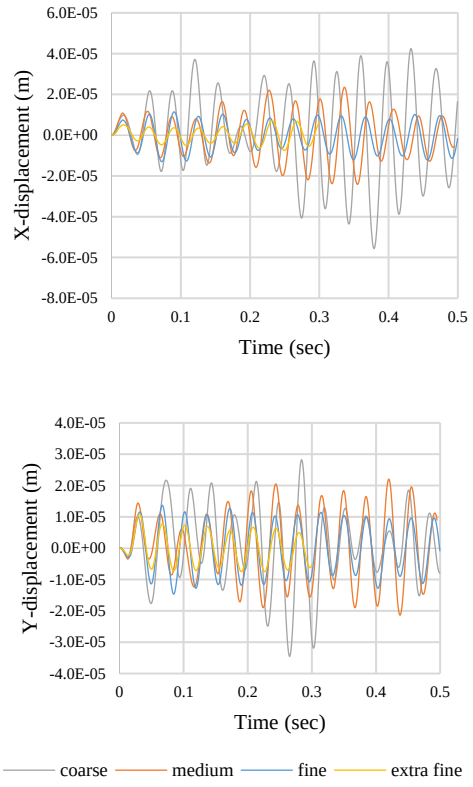

Fig. 16. Displacement vs. time of the middle point of the brass rod using one-way method.

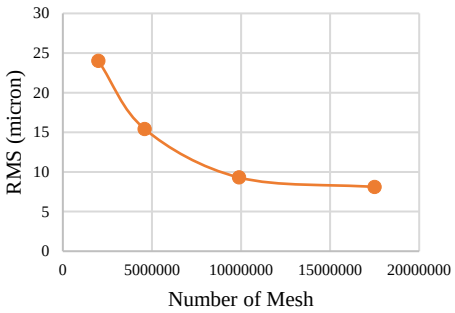

Fig. 17. Grid Independence diagram of the brass rod vibration simulations.

approximation (about 15% error) in order to reduce the simulations time. Figure 16 shows one-way simulations in several types of fluid volume meshing.

Figure 17 also shows the graph of grid independence based on the root means square of displacement of the rod middle point. Table 8 shows the frequency and average displacement of the brass rod with the one-way method. Considering the simulation time, it can be concluded that the fine-type mesh has the necessary accuracy and sufficiency for the correct estimation of displacement and frequency. Furthermore, using the one-way structure-fluid interaction method reduces the simulation time by 80%.

Table 8 Result of flow-induced vibration simulation of the brass rod using one-way method.

Mesh type	Frequency (Hz)	RMS (μm)	Simulation time (days)
Coarse	24.5	24.5	1
Medium	26.8	15.4	2
Fine	25.5	9.3	5
Extra fine	26.7	8.1	10

Table 9 Different types of meshing of fuel rod fluid volume

Mesh type	Number of divisions in $(r.\theta.z)$	Number of meshes	Time step (msec)
coarse	(27,54,1600)	2422400	0.18
medium	(30,72,2000)	4464000	0.15
fine	(37,110,2000)	8140000	0.12
Extra fine	(38,150,2500)	14250000	0.10

6.2 Fuel Rod Simulation Results

After validating the fluid-structure interaction model developed with the brass rod benchmark, the simulation of flow-induced vibration of the studied fuel rod is done. To investigate the effect of fuel rod supports on the frequency and amplitude of its

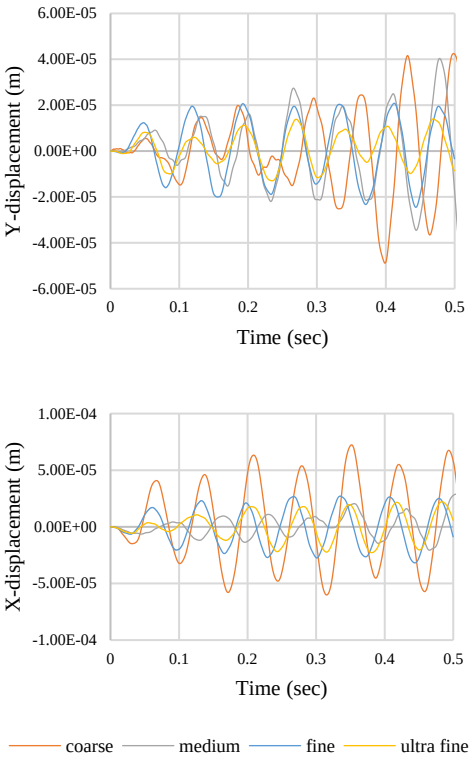

Fig. 18. Displacement vs. time of the middle point of the fuel rod without support.

vibrations, this simulation is done in two cases with the supports and without them. Based on Eqs. (8), the thickness of the first boundary layer to reach $y^+ \sim 1$ is 7 micron, and the time step is calculated based on Eqs. (9) for each mesh size. Also, to achieve grid independence, four types are considered for meshing the fluid volume of the studied problem, according to Table 9.

6.2.1 Fuel Rod Without Support

Similar to the simulation of the vibrations of the brass rod, the two-way interaction method is used for the coarse mesh first. After ensuring that the oscillation range is less than the height of the viscous sub-layer, the one-way interaction method is used to simulate other types of girds. Figure 18 shows the results of the simulation of the flow-induced vibrations of the fuel rod without support with the different numbers of meshes.

Figure 19 also shows the graph of grid independence based on the root mean square of the displacement range of the middle point of the rod. As seen, fine-type meshing has the necessary accuracy and adequacy for the correct displacement estimation.

6.2.2 Fuel Rod with Support

Now, the amplitude of the fuel rod vibrations with support is compared with the case without support. For this purpose, after ensuring the sufficiency of the

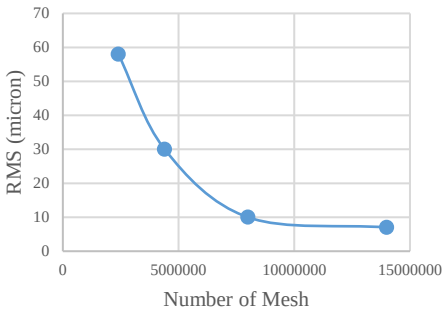

Fig. 19. Grid Independence diagram of the fuel rod vibration simulations.

number of extra fine mesh for the rod without support, the same number of mesh is used for the rod with support. Figure 20 shows the displacement of the middle points of the distances between the fuel rod supports.

Table 10 shows the frequency and average displacement of the fuel rod with and without support. As it is known, the range of fuel rod displacement has increased about 10 times in the case without supports.

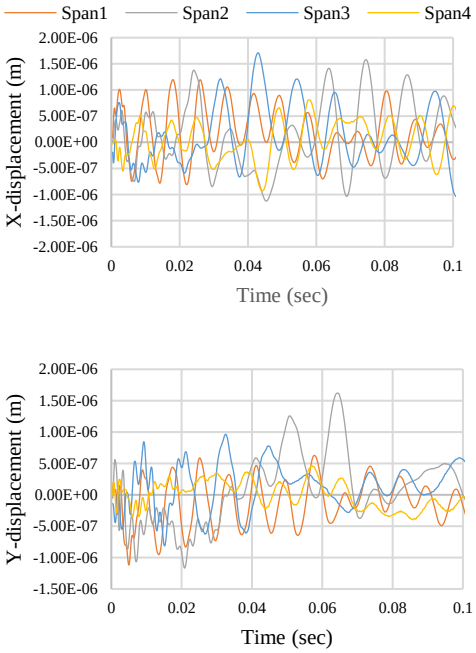

Fig. 20. Displacement vs. time of the middle points of the distances between fuel rod supports.

Table 10 flow-induced vibration simulations of the fuel rod without (a) and with (b) support.

Mesh type	Frequency (Hz)		RMS (micron)	
	(a)	(b)	(a)	(b)
fine	10	130	7	0.5-0.8

This shows how much the presence of supports will decrease the vibration range and consequently reduce the wear it causes. Also, the main natural frequency of the rod decreases when the rod loses contact with the supports and falls within the range of the reactor excitation frequency, i.e. 0 to 50 Hz, which should be avoided.

7. CONCLUSION

In this research, the simulation of the axial flow-induced vibrations of a specific fuel rod under elastic supports was studied to investigate the effect of these supports on the vibration of the rod. To simulate these vibrations, the numerical model of fluid-structure interaction implemented in ANSYS software was used. In this model, fluid flow was simulated using the LES turbulence model. First, the method of modeling the fluid-structure interaction in ANSYS software was validated using the results of the brass rod benchmark. Finally, the flow-induced vibration of the studied fuel rod was simulated and investigated in two cases with and without support.

By conducting a grid independence study, the results of the brass rod model showed that the grid is finer, the simulation results are closer to the test results. So that the difference between simulation and laboratory data has decreased from 9 microns (Nazari *et al.* 2019) to less than 2 microns in the present research. Considering the hardware limitations and long simulation time using the two-way fluid-structure interaction method, the one-way interaction method can be used with an acceptable approximation (about 15% error) in order to reduce the simulations time.

After validating the fluid-structure interaction model developed with the brass rod benchmark, the simulation results of the flow-induced vibration of the fuel rod showed that its displacement increased about 10 times in the case without support. This shows how much the presence of supports will reduce the vibration range and thus reduce the wear it causes. Also, the main natural frequency of the rod decreases when the rod loses contact with the supports and falls within the range of the reactor excitation frequency, i.e. 0 to 50 Hz, which should be avoided.

REFERENCES

Amirian, R., M. Talebi and Gh. R. Zarepoor (2022). Numerical model development of dummy fuel rod under new spacer grids and end constraints using experimental modal analysis. *Journal of Applied and Computational Sciences in Mechanics* (In Persian).

Celik, I. B., Z. N. Cehreli and I. Yavuz (2005). Index of resolution quality for large eddy simulations. *Journal of Fluids Engineering* 127, 949-958.

Chen, S. S. (1987). *Flow-Induced Vibration of Circular Cylindrical Structures*. Hemisphere Publishing Corp, Washington.

Chen, S. S. and M. W. Wambsganss (1972). Parallel-flow-induced vibration of fuel rods. *Nuclear Engineering and Design* 18(2), 253-278.

De Ridder, J., J. Degroote, K. Van Tichelen, P. Schuurmans and J. Vierendeels (2013). Modal characteristics of a flexible cylinder in turbulent axial flow from numerical simulations. *Journal of Fluids and Structures* 43, 110-123.

De Ridder, J., J. Degroote, K. Van Tichelen, P. Schuurmans and J. Vierendeels (2016). Predicting turbulence-induced vibration in axial annular flow by means of large-eddy simulations. *Journal of Fluids and Structures* 61, 115-131.

De Santis, D. and Shams, A. (2017). Numerical modeling of flow-induced vibration of nuclear fuel rods. *Nuclear Engineering and Design* 320, 44-56.

Eggels, J. G. M. (1995). Direct and large eddy simulation of turbulent flow in a cylindrical pipe geometry.

Georgiadis, N. J., D. P. Rizzetta and C. Fureby (2010). Large-eddy simulation: current capabilities, recommended practices, and future research. *AIAA journal* 48(8), 1772-1784.

IAEA-TECDOC-1454, (2004, November). Structural Behavior of Fuel Assemblies for Water Cooled Reactors. In *Proceedings of a Technical Meeting Held in Cadarache*, France.

IAEA Nuclear Energy Series No. NF-T-2.5, (2019), Review of Fuel Failures in Water Cooled Reactors (2006–2015), IAEA, Vienna.

Kanazawa, R. M. (1969). *Hydro-elastic Vibration of Rods in Parallel Flow*. Ph. D. Dissertation, University of Illinois at Urbana-Champaign, USA.

Kim, K. T. (2010). The effect of fuel rod supporting conditions on fuel rod vibration characteristics and grid-to-rod fretting wear. *Nuclear Engineering and Design* 240(6), 1386-1391.

Lesieur, M. (1997). Turbulence in Fluids Kluwer Academic Publishers.

Liu, Z. (2012). *Numerical simulation of fluid-structure interaction for elastic cylinders in axial flow*. Ph. D. Thesis, Polytechnic University, Hong Kong.

Nazari, T., A. Rabiee and H. Kazeminejad (2019). Two-way fluid-structure interaction simulation for steady-state vibration of a slender rod using URANS and LES turbulence models. *Nuclear Engineering and Technology* 51(2), 573-578.

Nazari, T., A. Rabiee and H. Kazeminejad (2020). Flow-induced vibration analysis of nuclear fuel rods using equivalent fuel element model. *Nuclear Engineering and Design* 363, 110639.

Païdoussis, M. P. (1965). *The Amplitude of Fluid-Induced Vibration of Cylinders in Axial Flow* (No. AECL-2225). Atomic Energy of Canada Ltd, Chalk River, Ontario (Canada).

Païdoussis, M. P. (1969). An experimental study of vibration of flexible cylinders induced by nominally axial flow. *Nuclear Science and Engineering* 35(1), 127-138.

Païdoussis, M. P. (1974). The dynamical behavior of cylindrical structures in axial flow. *Annals of Nuclear Science and Engineering* 1(2), 83-106.

Païdoussis, M. P. (1983). A review of flow-induced vibrations in reactors and reactor components. *Nuclear Engineering and Design* 74(1), 31-60.

Païdoussis, M. P. (1998). *Fluid-Structure Interactions: Slender Structures and Axial Flow*. Academic press.

Païdoussis, M. P. (2004). *Fluid-Structure Interactions: Slender Structures and Axial Flow*. Academic Press, London, UK.

Piomelli, U. and J. Chasnov (1996). *Turbulance and Transition Modeling*, Kluwer Academic Publishers, Chap. 7, 269-336.

Sagaut, P. (2001). Large eddy simulation for incompressible flows. Springer Science & Business Media.

Ter Hofstede, E., S. Kottapalli and A. Shams (2017). Numerical prediction of flow-induced vibrations in nuclear reactor applications. *Nuclear Engineering and Design* 319, 81-90.

Wilcox, D. C. (1998). *Turbulence Modeling for CFD*. La Canada, CA: DCW industries.

Wilcox, D. C. (2006). Turbulence Modeling for CFD. La Canada, CA: DCW Industries.

Wilson, R. J. and B. G. Jones (1983). Turbulent pressure-velocity measurements in a fully-developed concentric annular air-flow. *Journal of Vibration Acoustics Stress and Reliability in Design-Transactions of the ASME* 105(3), 345-354.

Wu, L., D. Lu and Y. Liu (2014). Experimental investigation on flow-induced vibration of fuel rods in supercritical water loop. *Science and Technology of Nuclear Installations*.

Zargar, S., R. A. Medina and L. Ibarra (2017, April). Effect of pellet-cladding bonding on the vibration of surrogate fuel rods. *In Proceedings of International High-level Radioactive Waste Management (IHLRWM 2017) Conference*, Charlotte, NC.

Zhang, X. (2011). *Numerical and experimental investigations on vibration of simulated CANDU fuel bundles subjected to turbulent fluid flow*. Library and Archives Canada, Ottawa.